IV.A.26 Digital Manufacturing of Gradient Meshed SOFC Sealing Composites with Self-Healing Capabilities

Dr. Kathy Lu (Primary Contact),
Christopher Story, Dr. W. T. Reynolds, Jr.
Virginia Polytechnic Institute and State University
213 Holden Hall, M/C 0237
Blacksburg, VA 24061
Phone: (540) 231-3225; Fax: (540) 231-8919
E-mail: klu@vt.edu

DOE Project Manager: Ayyakkannu Manivannan
Phone: (304) 285-2078
E-mail: Ayyakkannu.Manivannan@netl.doe.gov

Objectives

- Use three dimensional printing (3DP) technique to build a shape memory alloy (SMA) skeleton for the seal on the seal-interconnect side.
- Use glass to fill the meshed SMA structure and transition into pure glass seal on the electrolyte side.
- Provide gradient coefficient of thermal expansion (CTE) to reduce the thermal stress.
- Further reduce the thermal stresses in the seal by SMA phase transformation toughening.
- Provide self-healing of cracks by SMA shape recovery during solid oxide fuel cell (SOFC) thermal cycling.

Accomplishments

- Developed multiple AUTOCAD drawings of wire structure and 3D printed multiple configurations of the wire structure.
- Synthesized new composition TiNiHf alloy by gas atomization method. The new alloy composition has a slightly higher Ni concentration to facilitate a more uniform microstructure.
- Extensive work was carried out for the optimization of the parameters of the three dimensional printing technique. An emulsion binder was developed for the proposed TiNiHf alloy powder.
- SMA/glass composite was produced. Neutron diffraction provided 0.001 Å measurement resolution for the TiNiHf alloy lattice parameter change during thermal cycling. Austenite to martensite phase transformation can be observed in-situ by neutron diffraction.
- SMA alloy demonstrated the ability of reducing the thermal stresses in the seal by SMA phase transformation toughening.
- Dilatometry has been used to measure the thermal expansion coefficient of the commercial cell electrolyte and interconnect. The proposed SMA/glass has the potential to bridge the thermal expansion coefficient mismatch between the cell components.

Introduction

SOFC seals have a demanding set of imposed performance criteria. Of particular importance is the ability to seal between metallic and ceramic components with differing CTEs and do so while being electrically insulating and exposed to temperature transients from room temperature up to ~650-950ºC. A major roadblock to long-term SOFC operation has been gas leakage through the seal caused by multiple heating and cooling cycles (thermal cycling). The gas seal cracks because the metal and ceramic components that are sealed together shrink and expand differently (CTE mismatch), causing high stresses in the seal.

A host of seal materials have been explored, such as FeCrAlY, DuraFoil, Si-C-N polymers, ceramic and metallic fillers, mica, and glass-ceramic fibers (1-6). However, interdiffusion and durability of some of these materials in the oxidizing and reducing environments of SOFC are unknown. Some of these seals require compressive loads or have unknown leakage protection capability. An improved glass matrix should be selected to avoid the above problems. Also, cracking during thermal cycling can be avoided by the integration of a second phase which is a better match to the thermal expansion of the metallic interconnect. An SMA has a CTE close to that of the interconnect and presents the possible benefit of crack healing because of the shape memory behavior when heated.

Approach

We used gas atomization to obtain different size particles and adjusted the SMA composition to a higher Ni content in the process of optimizing the SMA alloy composition. After the SMA is fabricated, the powder was processed to -635 mesh. After that, the SMA alloy was 3D printed into a wire structure. 3D printing allows creating wire diameters of 200-500 µm and printing layers that are 25-100 µm thick. Since the 3DP technique was newly applied to the TiNiHf system, the printing parameters and the binders all need to be re-examined. We have systematically analyzed all the 3DP

parameters and identified three key parameters that need to be optimized: binder type, binder saturation level, and printing layer thickness. The SMARTS system in the Lujan Center at Los Alamos National Laboratory, New Mexico was used for neutron diffraction of glass/SMA composite. Samples were placed free standing on a graphite base in the chamber of a vacuum furnace. They were heated at 15°C/min to 800°C and then cooled at different rates. The glass/SMA sample was cooled first at 5°C/min to 375°C and then held for approximately 30 minutes to achieve a neutron detection count of 1.5×10^3 Ah. The sample was then cooled in 10°C and 20°C steps at 5°C/min for more diffraction patterns. The same glass/SMA sample was heated again to 800°C and then cooled at 30°C/min to a first diffraction temperature of 350°C and cooled in 25°C and 10°C steps. A similar temperature profile was conducted on the SMA slivers without glass, with the exception that the cooling rate was at 15°C/min. For the CTE measurements, a push rod dilatometer (Orton 1600B, Edward Orton, Jr. Ceramic Foundation, Westerville, Ohio) was used. We obtained commercial SOFC electrolyte, Sc-stabilized ZrO_2, from Ceramatec (Salt Lake City, Utah) and the stainless steel interconnect from ATI Allegheny Ludlum (Pittsburgh, Pennsylvania) under the trade name E-BRITE®. The temperature range studied was from room temperature to 800°C to mimic the operation condition of actual SOFCs.

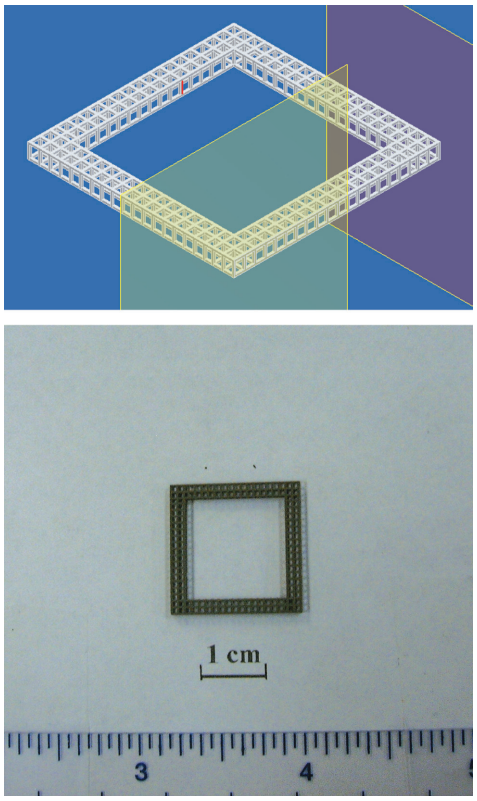

FIGURE 1. AUTOCAD Wire Mesh Design (top) and 3D Printed Wire Mesh (bottom)

Results

New composition TiNiHf alloy powder has been successfully synthesized by gas atomization. As desired, the atomic percent of Ni increased by 1% in comparison to the arc-melted TiNiHf composition reported last year.

Extensive work has been carried out for the 3DP parameter optimization. In an effort to increase the mesh strength, the binder saturation level was increased several times from 55% to 170%. Intricate wire structures were printed as shown in Figure 1. An emulsion binder was developed for the proposed TiNiHf alloy powder. The viscosity of the emulsion binder is much lower than that of the existing binder, making it suitable to be used in the 3D printing machine (Figure 2). The particles bound by the 40 vol% emulsion binder solution could not be broken with tweezers.

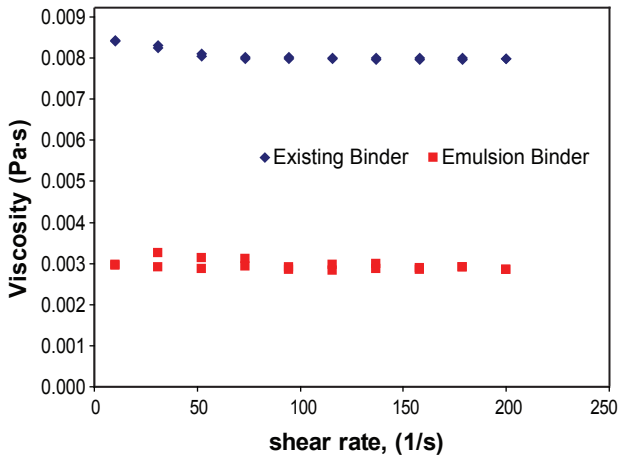

FIGURE 2. Viscosity Comparison of the Existing Binder and the Emulsion Binder

Neutron diffraction provides 0.001 Å measurement resolution for the TiNiHf alloy lattice parameter change. The thermal stress generated from the glass matrix shifts the SMA austenite to martensite phase transformation temperature to a higher temperature during cooling. The thermal expansion coefficient at the lattice level from the neutron diffraction matches well with the CTE measurement from the dilatometry. Figure 3 is a neutron diffraction pattern during the austenite to martensite transition. The thick arrow points to the austenite (110) peak while the dotted arrow points to a martensite double peak. As shown in Figure 3, the martensite peak was barely visible at 180°C. As the temperature was decreased to 162°C and 124°C, the martensitic (101) and (020)/(012) double peak intensity kept increasing, indicating the austenite to martensite

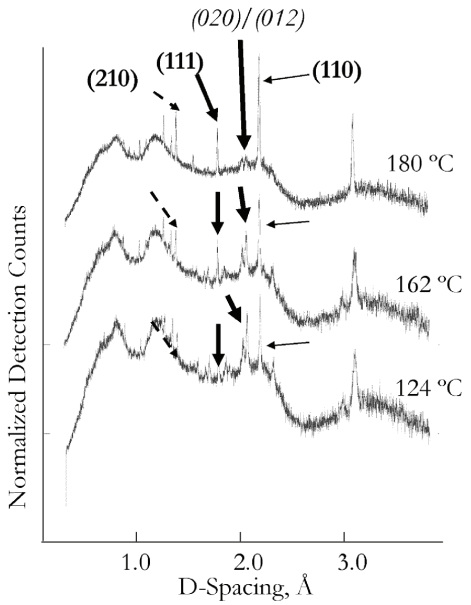

FIGURE 3. Neutron Diffraction Pattern from the Glass/SMA Sample at 180°C, 162°C, and 124°C

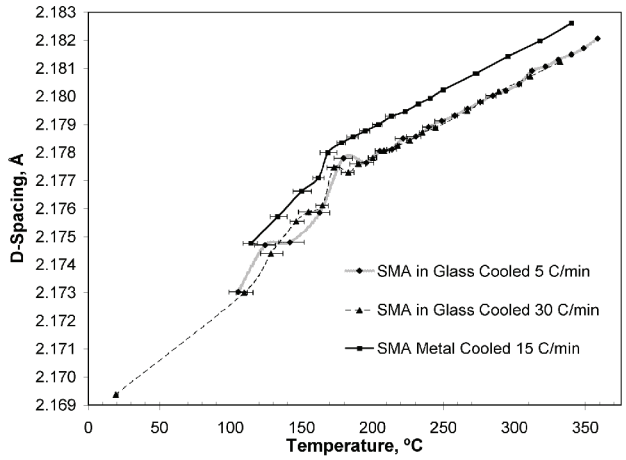

FIGURE 4. D-Spacing of the (110) Austenite Peak during Cooling

phase transformation process ((020) and (012) peaks are located on the right side of the double peak but are too close to be resolved).

D-spacing of the (110) austenite peak is plotted in Figure 4 for the three samples at different temperatures. The (110) d-spacing for the SMA alloy without glass is approximately 0.001 Å higher than that in glass during cooling above the martensitic transition. The curves are identical for the slow cooled and fast cooled SMA/glass samples and are both parallel to that of the SMA sample. The only likely cause is the thermal stress induced phase transformation change. However, there is one aspect that cannot be explained. The thermal stresses from the glass should increase the SMA d-spacing because the metal has a higher CTE and tends to shrink more during cooling. This can be caused by the metastable nature of the glassy phase but needs to be further studied.

Dilatometry has been used to measure the CTEs of the commercial cell electrolyte and interconnect. The CTE of the E-BRITE® stainless steel interconnect is $16.8x10^{-6}$/K. The CTE of the scandia stabilized zirconia is $9.5x10^{-6}$/K. For both stainless steel and ZrO_2, the CTEs are fairly consistent across the measurement temperature range of room temperature to 800°C. The CTE of the glass is $7.02x10^{-6}$/K between 40°C and 500°C, $32.0x10^{-6}$/K between 500°C and 700°C, and $21.4x10^{-6}$/K between 700-800°C; the overall CTE is $13.9x10^{-6}$/K. The CTE of SMA is $12.5x10^{-6}$/K. These measurements confirm the need for CTE match at various temperatures for different SOFC components. These measurements provide quantitative CTE difference comparison for continuing seal composition optimization.

Conclusions

1. TiNiHf alloy has been successfully synthesized by gas atomization with the desired particle size for the 3DP process. This solves the SMA ductility issue encountered during the SMA alloy milling.
2. The parameters for the 3DP process have been evaluated and optimized. A new binder has been identified to match with the specific chemistry of the SMA particles.
3. Neutron diffraction shows to be an extremely useful tool in providing information regarding the austenite to martensite phase transformation, SMA alloy lattice constant change, and the corresponding thermal stress from the glass matrix. It pinpoints regions of SMA phase transformation and the thermal stress effect under simulated SOFC thermal cycles.

Future Directions

- Detailed glass and SMA composition optimization is needed.
- Further understanding of the glass and SMA interaction is needed.
- Composite seal performance should be studied with the optimized seal design.

FY 2007 Publications/Presentations

1. K. Lu, C. Story, and W. T. Reynolds, "Glass/Shape Memory Alloy Composite Study for Solid Oxide Electrolyzer/Fuel Cell Applications," 31st International Cocoa Beach Conference & Exposition on Advanced Ceramics and Composites, January 21-26, 2007, Daytona Beach, FL.

2. C. Story, W. Reynolds, and K. Lu, "Shape Memory Alloy/Glass Composite Gas Seal for Solid Oxide Fuel Cells," 2007 TMS Annual Meeting & Exhibition, February 25, 2007 – March 1, 2007, Orlando, FL.

3. C. Story, K. Yu, K. Lu, and W. T. Reynolds, "Self-Healing Composite Seals for Solid Oxide Electrolyzer/Fuel Cells," Deans' Form on Energy Security and Survivability, October 16, 2006, Blacksburg, VA.

References

1. K. S. Weil, J. Y. Kim and J. S. Hardy, "Reactive Air Brazing: A Novel Method of Sealing SOFCs and Other Solid-State Electrochemical Devices," *Electrochemical and Solid-State Letters*, 8(2), A133-A136, 2005.

2. K. S. Weil and J. S. Hardy, "Development of a Compliant Seal for Use in Planar Solid Oxide Fuel Cells," *28th International Conference on Advanced Ceramics and Composites*, E. Lara-Curzio and M. J. Readey, eds. 25, pp. 321-326, American Ceramic Society, Cocoa Beach, FL, 2004.

3. Y.-S. Chou and J. W. Stevenson, "Long-Term Thermal Cycling of Phlogopite Mica-Based Compressive Seals for Solid Oxide Fuel Cells," *Journal of Power Sources*, 140, 340–345, 2005.

4. M. Bram, S. Reckers, P. Drinovac, J. Monch, R. W. Steinbrech, H. P. Buchkremer and D. Stover, "Deformation Behavior and Leakage Tests of Alternate Sealing Materials for SOFC Stacks," *Journal of Power Sources*, 138, 111–119, 2004.

5. S. Taniguchi, M. Kadowaki, T. Yasuo, Y. Akiyama, Y. Miyake and K. Nishio, "Improvement of Thermal Cycle Characteristics of a Planar-Type Solid Oxide Fuel Cell by Using Ceramic Fiber as Sealing Material," *Journal of Power Sources*, 90, 163–169, 2000.

6. J. W. Fergus, "Sealants for Solid Oxide Fuel Cells," *Journal of Power Sources*, 147, 46-57, 2005.